

Title	Nondispersive electron transport in Alq ₃
Author(s)	Malliaras, George G.; Shen, Yulong; Dunlap, David H.; Murata, Hideyuki; Kafafi, Zakya H.
Citation	Applied Physics Letters, 79(16): 2582-2584
Issue Date	2001-10-15
Type	Journal Article
Text version	publisher
URL	http://hdl.handle.net/10119/4532
Rights	Copyright 2001 American Institute of Physics. This article may be downloaded for personal use only. Any other use requires prior permission of the author and the American Institute of Physics. The following article appeared in G. G. Malliaras, Y. Shen, D. H. Dunlap, H. Murata, Z. H. Kafafi, Applied Physics Letters, 79(16), 2582-2584 (2001) and may be found at http://link.aip.org/link/?APPLAB/79/2582/1
Description	

Nondispersive electron transport in Alq₃

George G. Malliaras,^{a)} Yulong Shen, and David H. Dunlap^{b)}

Department of Materials Science and Engineering, Cornell University, Ithaca, New York 14853

Hideyuki Murata^{c)} and Zakya H. Kafafi

Optical Sciences Division, U.S. Naval Research Laboratory, Washington, DC 20375

(Received 9 April 2001; accepted for publication 20 August 2001)

We have studied room temperature electron transport in amorphous films of tris (8-hydroxyquinolinolato) aluminum (III) (Alq₃) with the time-of-flight technique. Nondispersive photocurrent transients indicate the absence of intrinsic traps in well-purified films. Exposure of the films to ambient atmosphere results in highly dispersive transport, indicating that oxygen is a likely candidate for a trapping site. The mobility was found to obey the Poole–Frenkel law. We use the correlated disorder model to determine an effective dipole moment for Alq₃, and the corresponding meridional to facial isomeric ratio. © 2001 American Institute of Physics.

[DOI: 10.1063/1.1410343]

Since the first report of an organic light emitting diode (OLED),¹ a dramatic improvement has been achieved in the efficiency and lifetime of these devices,² which has recently led to the commercialization of OLED-based flat panel displays. This fast-paced progress is partly enabled by our understanding of the charge transport properties of organic semiconductors.³ Tris (8-hydroxyquinolinolato) aluminum (III) (Alq₃) was the electron transporter and emitter in the first OLED¹ and still remains one of the most widely used. Early attempts to model its transport characteristics employed band models with a distribution of trapping levels below the conduction band.⁴ Such treatments, however, fail to capture the identifying characteristics of organic materials. Due to the structural disorder in Alq₃ and other amorphous glasses, transport states are energetically disordered and spatially localized. The mobility μ in Alq₃ is not constant, but electric field dependent according to:^{5–7}

$$\mu = \mu_0 \exp(\beta\sqrt{E}), \quad (1)$$

where μ_0 is the (extrapolated) zero field mobility and β the so-called Poole–Frenkel (PF) factor. Reported values for μ_0 range from 10^{-9} to 10^{-7} cm²/V s depending on sample preparation, while β is of the order of 10^{-2} (cm/V)^{0.5}, giving an electron mobility between 10^{-6} and 10^{-5} cm²/V s under typical OLED operating conditions.⁶ Recently, Ioannidis *et al.*⁸ have shown that Eq. (1) can account for the field and thickness dependence of the current in Alq₃ films, as is also the case for conjugated polymers.⁹

There is, however, considerable evidence for the presence of deep traps in Alq₃ films. Dispersive time-of-flight (TOF) measurements have been interpreted to arise from bulk trapping,⁷ and thermally stimulated current studies seem to reveal trapping sites with a depth of 0.8 eV.¹⁰ It is impor-

tant to understand the nature of trapping since it may lead to a buildup of space charge which results in device degradation.

Electron transport in amorphous organic films takes place by hopping in a manifold of localized states which is composed of the lowest unoccupied molecular orbitals of each molecule. The distribution of energies is normally assumed to be Gaussian, with a width σ that is of the order of 0.1 eV.¹¹ It has been shown from simulations that a packet of carriers propagating in such a system can quickly reach thermal quasiequilibrium at room temperature.¹¹ This leads to nondispersive spatial evolution of the carrier packet, which is indicative of trap-free charge transport. This behavior has been observed in a variety of organic semiconductors.³

In this context, electron traps are unoccupied energy levels positioned lower than the transport manifold by at least a few σ . Their introduction will result in the removal of carriers from the transport manifold and will lead to dispersive current-time curves. Traps may arise due to chemical impurities such as molecular oxygen, which can be removed by proper purification. Traps may also be present for intrinsic reasons, however, as in the formation of dimers in polyvinylcarbazole.¹² In the latter case purification will not improve the transport characteristics. In Alq₃ films it has not been clear whether the traps are intrinsic or extrinsic in nature.

In this letter we report results from TOF measurements that show nondispersive electron transport in well-purified Alq₃, indicative of the absence of intrinsic traps. Exposure of the Alq₃ film to atmosphere results in highly dispersive transport, indicating that oxygen is a likely candidate for a trap. The electric field dependence of the mobility in Alq₃ is investigated and discussed.

High purity Alq₃ was purchased from H.W. Sands Corp. Part of it was used as-received, while the rest was purified three times by train sublimation. For the transport measurements, films were prepared on prepatterned indium-tin-oxide (ITO) coated glass substrates. The ITO substrates were cleaned by sonication in a deionized water bath, dried and exposed to UV/ozone at slightly elevated temperatures. Sub-

^{a)}Author to whom correspondence should be addressed; electronic mail: george@ccmr.cornell.edu

^{b)}Permanent address: Department of Physics and Astronomy, University of New Mexico, Albuquerque, NM 87131.

^{c)}Permanent address: Department of Chemistry, Imperial College, London SW7 2AY, UK.

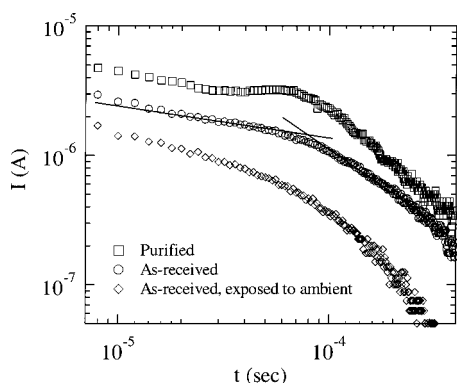


FIG. 1. Time-of-flight electron transients from the as-received (circles) and purified (squares) Alq_3 samples. The diamonds are data from the as-received sample after exposure to atmosphere. The lines are guides to the eye and are meant to indicate the change in slope upon arrival of photoexcited electrons to the opposite electrode.

sequently, they were introduced into a glove box, where all the preparation steps took place in a dry nitrogen atmosphere with <1 ppm oxygen and moisture concentrations. The organic films were deposited by vacuum sublimation at 10^{-6} mbar. The thickness of the films, measured by profilometry, was in the range of $8 \mu\text{m}$. The device preparation was completed by the deposition of a semitransparent aluminum (Al) layer which defined six devices per substrate each with an active area of 3 mm^2 .

The mobilities were measured by the photoinduced TOF technique.¹³ The sample was transported and held in a custom-made vacuum container at $T=294$ K without any exposure to the atmosphere. The measurements were then repeated after exposure of the sample to the atmosphere. A nitrogen laser ($\lambda=337$ nm) with a 10 ns pulse width was used as the excitation source, and was incident on the sample through the ITO electrode that was biased negative with respect to the Al electrode. The dark current was found to be negligible under this bias configuration indicating that ITO and Al act as noninjecting (“blocking”) contacts for electron and hole injection, respectively. All TOF traces were recorded in the single shot regime. The intensity of the laser was kept sufficiently low to avoid space charge effects and the response time of the circuit was kept well below the transit time. All six devices on the same substrate were found to exhibit similar TOF traces. Although not the subject of the present investigation, we should also remark that hole transport was found to be nondispersive, having a mobility of the order of $10^{-8} \text{ cm}^2/\text{V s}$, in agreement with that reported in the literature.⁷

A typical TOF trace in the as-received Alq_3 film is shown in Fig. 1 (circles). The dispersive character of transport is evident in the continuous decay of the photocurrent (I), which progresses until $t \approx 8 \times 10^{-5}$ s. At that time, enough charge has reached the opposite electrode to cause a change in slope. The behavior is typical for dispersive transport. Exposure of the sample to ambient atmosphere for just 2 h has a notable effect on the magnitude and the slope of the photocurrent, which decreases and decays at a faster rate (diamonds). After overnight exposure, the photocurrent became indiscernible (not shown here), suggesting a dramatic increase in charge trapping.

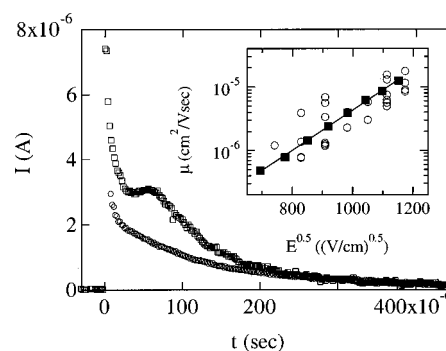


FIG. 2. Time-of-flight electron transients from the as-received (circles) and purified (squares) Alq_3 samples. Inset: electric field dependence of mobility of the as-received (circles) and purified (squares). The line is a fit to Eq. (1).

A typical TOF trace for the purified Alq_3 is also shown in Fig. 1 (squares). The behavior of the photocurrent is distinctly different from that of the as-received Alq_3 sample. After an initial decay the photocurrent shows a plateau, indicating that the photoinjected electrons reach thermal quasiequilibrium with the transport manifold in Alq_3 . This non-dispersive evolution of the electron packet is the signature of trap-free transport, and supports the conclusion that the dispersive transport in as-received Alq_3 is caused by an extrinsic mechanism. Upon exposure of the purified film to the atmosphere, the TOF traces again became very dispersive (not shown here), in a similar fashion to the as-received sample.

The difference between the as-received and purified samples is better illustrated in Fig. 2. The circles are data from the as-received sample, which show the characteristic featureless decay associated with dispersive transport. In sharp contrast, the TOF trace from the purified sample (squares) indicates trap-free hopping transport. The tail of the photocurrent exhibits the characteristic anomalous diffusion observed in amorphous glasses. For the curve shown in Fig. 1, the tail-broadening parameter¹⁴ $W=0.5$, comparable to that in the electron transporting glass NTDL.¹⁵

The field dependence of the mobility for the purified sample is shown in the inset of Fig. 2 (filled squares). The mobility was determined from the relationship $\mu = L^2/(t_{\text{TR}} V)$, where L is the sample thickness, V is the applied voltage, and t_{TR} is the transit time.¹³ The mobility is found to obey Eq. (1) for $\mu_0 = 2.9 \times 10^{-9} \text{ cm}^2/\text{V s}$ and $\beta = 7.3 \times 10^{-3} (\text{cm}/\text{V})^{0.5}$ consistent with literature values.¹⁶

Although Eq. (1) is the well known PF law,¹⁶ the mechanism behind the electric field dependence of mobility in amorphous glasses is recognized *not* to be due to the PF effect, but is instead caused by long-range spatial correlations in the energetic disorder characterizing the transport manifold.¹⁷ Site-energy correlations arise in a natural manner as a result of the unscreened electrostatic forces felt by the injected charges due to the nonvanishing multipole moments of the surrounding molecules.¹⁸ The longest correlation, arising from the charge–dipole interaction, has been shown to give rise to a PF field dependence in the range of fields probed by experiment.^{19,20} From computer simulations of hopping transport on a simple cubic lattice of randomly oriented dipoles,²⁰ it has been shown that the PF slope obeys the phenomenological expression

$$\beta = 0.78 \cdot (e\alpha/\sigma)^{1/2} \cdot [(\sigma/kT)^{3/2} - 1.97], \quad (2)$$

where the variance

$$\sigma^2 = (1/3) \cdot 16.53 \cdot (pe/4\pi\epsilon\alpha^2)^2, \quad (3)$$

depends on the magnitude of the dipole moment p ,²¹ and α is the lattice constant. Since it is the decay of the site-energy correlation function over lengths which are large compared to the nearest-neighbor hopping distance which causes the \sqrt{E} field dependence,²² local fluctuations in the dipole density due to molecular orientation and packing have little effect on the PF factor. To determine beta it is sufficient, therefore, to substitute an effective lattice constant

$$\alpha = [459 / (1.3 \times 6.02 \times 10^{23})]^{1/3} = 8.4 \times 10^{-8} \text{ cm}, \quad (4)$$

determined from the Alq₃ density of 1.3 g/cm³ and molecular weight of 459 g/mole. To calculate σ , we note that Eq. (2) is a cubic equation in the dimensionless variable $x = (\sigma/kT)^{1/2}$, such that

$$x = \{[\beta(kT/e\alpha)^{1/2}/(0.78)]x + 1.97\}^{1/3} \\ = (5.14x + 1.97)^{1/3}. \quad (5)$$

The solution $x = 2.44$ may be found by iteration, from which it follows that

$$\sigma = (8.64 \times 10^{-5} \text{ eV/K}) \cdot (294 \text{ K}) \cdot (2.44)^2 = 0.15 \text{ eV}. \quad (6)$$

Substituting the values for σ and α determined above in Eq. (3), and taking a dielectric permittivity $\epsilon = 3.5 \cdot \epsilon_0$, we find a representative dipole moment $p = 4.9 \text{ D}$. In comparison, the meridional and facial isomers of Alq₃ have dipole moments $p_m = 4.4$ and $p_f = 7.7 \text{ D}$, respectively.²³ Since the variance of the Gaussian density of states is proportional to the square of the dipole moment, we may calculate the meridional to facial isomeric ratio r from the weighted average

$$p^2 = (r/r + 1) \cdot p_m^2 + (1/r + 1) \cdot p_f^2, \quad (7)$$

assuming that the two isomers contribute independently. From Eq. (7) we find a value of $r = 7.4(15:2)$. The relatively small presence of the facial isomer is consistent with infrared matrix-isolation studies combined with *ab initio* calculations.²⁴

For the sake of comparison, values of the mobility calculated for the as-received sample are shown in the inset of Fig. 2 (circles). The transit time was determined from the inflection point on a $\log(I) - \log(t)$ plot.²⁵ The multiple data points are meant to indicate the degree of variation in successive measurements, which is partly due to the uncertainty in calculating t_{TR} . The mobility is comparable to that in the purified sample and the PF factor is similar. The former is to be expected, for in the case of dispersive transport the inflection point corresponds to arrival of the fastest carriers to the opposite electrode. The PF factor should be the same in any event because it represents a field-induced reduction of the time the moving charges spend trapped in a hierarchy of spatially broad energetic valleys arising from the correlated disorder.²² Punctuating these valleys with localized traps will

increase the magnitude of the escape time, but will not affect its relative field dependence.²⁶

In conclusion, we have observed nondispersive electron transport in a well-purified Alq₃ film, with no intrinsic traps. Exposure to ambient atmosphere introduced traps, which gave rise to dispersive transport. The mobility was found to obey the Poole-Frenkel law. By comparing the PF slope with that predicted by the correlated disorder model, we determined an effective dipole moment for Alq₃, and the corresponding meridional to facial isomeric ratio.

This project was partly supported with a Grant from the National Science Foundation (Knowledge and Distributed Information Award No. DMR-9980100). H.M. and Z.H.K. gratefully acknowledge financial support from the Defense Advanced Research Projects Agency and the Office of Naval Research. The authors are grateful to Ralph Young for his insightful comments.

¹C. W. Tang and S. A. VanSlyke, Appl. Phys. Lett. **51**, 913 (1987).

²See, for example, J. C. Scott and G. G. Malliaras, in *Conjugated Polymers*, edited by G. Hadziioannou and P. F. van Hutten, (Wiley, New York, 1999).

³P. M. Borsenberger and D. S. Weiss, *Organic Photoreceptors for Xerography* (Marcel Dekker, New York, 1998).

⁴P. E. Burrows, Z. Shen, V. Bulovic, D. M. McCarty, S. R. Forrest, J. A. Cronin, and M. E. Thompson, J. Appl. Phys. **79**, 7991 (1996).

⁵R. G. Kepler, P. M. Beeson, S. J. Jacobs, R. A. Anderson, M. B. Sinclair, V. S. Valencia, and P. A. Cahill, Appl. Phys. Lett. **66**, 3618 (1995).

⁶B. J. Chen, W. Y. Lai, Z. Q. Gao, C. S. Lee, S. T. Lee, and W. A. Gambling, Appl. Phys. Lett. **75**, 4010 (1999).

⁷S. Naka, H. Okada, H. Onnagawa, Y. Yamaguchi, and T. Tsutsui, Synth. Met. **111**, 331 (2000).

⁸A. Ioannidis, E. Forsythe, Y. Gao, M. W. Wu, and E. M. Conwell, Appl. Phys. Lett. **72**, 3038 (1998).

⁹G. G. Malliaras, J. R. Salem, P. J. Brock, and J. C. Scott, Phys. Rev. B **58**, R13411 (1999).

¹⁰T. Mori, S. Miyake, and T. Mizutani, Jpn. J. Appl. Phys., Part 1 **34**, 4120 (1995).

¹¹H. Bässler, Phys. Status Solidi B **175**, 15 (1993).

¹²M. Fujino, W. Kanazawa, H. Mikawa, S. Kusabayashi, and M. Yokoyama, Solid State Commun. **49**, 575 (1984).

¹³A. R. Melnyk and D. M. Pai, in *Determination of Electronic and Optical Properties, Physical Methods of Chemistry Series*, 2nd ed. edited by B. W. Rossiter and R. C. Baetzold (Wiley, New York, 1993), Vol. VIII.

¹⁴For definition see, L. B. Schein, Philos. Mag. B **65**, 795 (1992).

¹⁵P. M. Borsenberger, W. T. Gruenbaum, and E. H. Magin, Phys. Status Solidi B **190**, 555 (1995).

¹⁶H. H. Poole, Philos. Mag. **33**, 112 (1916).

¹⁷Y. N. Gartstein and E. M. Conwell, Chem. Phys. Lett. **245**, 351 (1995).

¹⁸S. V. Novikov and A. V. Vannikov, J. Phys. Chem. **99**, 14573 (1995).

¹⁹D. H. Dunlap, P. E. Parris, and V. M. Kenkre, Phys. Rev. Lett. **77**, 542 (1996).

²⁰S. V. Novikov, D. H. Dunlap, V. M. Kenkre, P. E. Parris, and A. V. Vannikov, Phys. Rev. Lett. **81**, 4472 (1998).

²¹R. H. Young, Philos. Mag. B **72**, 435 (1995).

²²D. H. Dunlap, P. E. Parris, and V. M. Kenkre, J. Imaging Sci. Technol. **43**, 437 (1999).

²³G. P. Kushto and Z. H. Kafafi (unpublished).

²⁴G. P. Kushto, Y. Iizumi, J. Kido, and Z. H. Kafafi, J. Phys. Chem. A **104**, 3670 (2000).

²⁵H. Scher and E. W. Montroll, Phys. Rev. B **12**, 2455 (1975).

²⁶S. V. Novikov, D. H. Dunlap, and V. M. Kenkre, Proc. SPIE **3471**, 181 (1998).